Electrical synapses formed by connexin36 regulate inhibition- and experience-dependent plasticity

Friso Postma[a,1], Cheng-Hang Liu[b,1], Caitlin Dietsche[b], Mariam Khan[b], Hey-Kyoung Lee[b], David Paul[a], and Patrick O. Kanold[b,c,2]

[a]Department of Neurobiology, Harvard Medical School, Boston, MA 02115; and [b]Department of Biology and [c]Institute for Systems Research, University of Maryland, College Park, MD 20742

Edited* by Carla J. Shatz, Stanford University, Stanford, CA, and approved June 29, 2011 (received for review January 7, 2011)

The mammalian brain constantly adapts to new experiences of the environment, and inhibitory circuits play a crucial role in this experience-dependent plasticity. A characteristic feature of inhibitory neurons is the establishment of electrical synapses, but the function of electrical coupling in plasticity is unclear. Here we show that elimination of electrical synapses formed by connexin36 altered inhibitory efficacy and caused frequency facilitation of inhibition consistent with a decreased GABA release in the inhibitory network. The altered inhibitory efficacy was paralleled by a failure of theta-burst long-term potentiation induction and by impaired ocular dominance plasticity in the visual cortex. Together, these data suggest a unique mechanism for regulating plasticity in the visual cortex involving synchronization of inhibitory networks via electrical synapses.

gap junctions | development | cannabinoid receptor 1 | synchrony

Synaptic interactions in the mammalian brain are sculpted by experience, particularly during "critical periods" in development. Accumulating evidence suggests that inhibitory neurons play a crucial role in reshaping neural networks in response to sensory perturbations (1). Inhibitory neurons in many areas of the brain, including the cerebral cortex, are coupled via gap junctions containing connexin36 (Cx36), which allow subthreshold fluctuations in membrane potential to spread between cells and promote synchrony of firing (2–5). Cx36-null mice (Cx36KO) display decreased coherence of rhythmic activity in populations of cortical interneurons in brain slices and decreased strength of evoked cortical inhibition in vivo (6–8). Similar effects of Cx36 signaling might underlie the behavioral deficits in cerebellar learning tasks in Cx36KO (7). However, the possible functions of Cx36 in sensory cortical development and plasticity are unknown.

A common model for experience-dependent synaptic modification is ocular dominance (OD) plasticity of visual cortex. In the visual cortex, decreasing neural activity in one eye (monocular deprivation; MD) leads to weakening and removal of connections representing the deprived eye (DE) and strengthening and expansion of connections representing the nondeprived eye (NDE; refs. 9–13). These manipulations are particularly effective during the critical period, which extends from postnatal day (P) 19 to ~P55 and peaks at ~P25–28 in mice (11, 14, 15). Both inhibition and synaptic plasticity mechanisms, such as long-term potentiation (LTP) and long-term depression (LTD), play a key role in OD plasticity, and inhibition can alter synaptic plasticity (1, 16, 17). Cx36 is present in most cortical layers during the critical period for OD plasticity (6). We therefore investigated to what degree Cx36 controls inhibitory function and, consequently, synaptic and OD plasticity.

Here we report altered dynamics of the evoked inhibitory synaptic currents in mice lacking Cx36, such that there is a reduction when probed at low-frequency stimulation but a facilitation at higher frequencies. Furthermore, Cx36-mediated coupling is required for the induction of theta-burst stimulation (TBS)-induced LTP. However, pairing LTP and AMPA/NMDA ratios were normal in Cx36KO, suggesting that the cellular mechanisms for LTP or excitatory synaptic transmission are not grossly affected. Correlated with the lack of TBS-LTP, Cx36KOs showed paradoxically inverted OD plasticity for the NDE. Chronic application of AM251, a cannabinoid receptor 1 (CB1) antagonist that can increase GABA release, rescued the OD defect. Thus, electrical coupling has profound effects on the temporal dynamics of inhibition and is a critical aspect of OD plasticity.

Results

Cx36 Alters the Dynamics of Stimulus-Evoked Inhibition. To investigate the influence of Cx36 on cortical function and plasticity, we first investigated inhibitory network function in Cx36KOs. Cx36 has been shown to electrically couple individual inhibitory neurons (6), and this coupling promotes synchrony of firing (2–5). However, the effect of coupling on the functional dynamics of inhibitory networks and their postsynaptic targets is unknown. We used patch-clamp recordings to determine the properties of the inhibitory network in Cx36KOs (6). In these mice, the coding region for Cx36 was replaced with a construct for β-gal and alkaline phosphatase. Because interneurons in Cx36 heterozygotes (HETs) form electrical and chemical connections similar to wild-type (WT) animals (18, 19), we compared putative changes in inhibitory synaptic transmission in KO cells to their HET counterparts, thereby controlling for possible effects of reporter gene expression.

We recorded inhibitory postsynaptic currents (IPSCs) from layer 4 (L4) neurons in mouse visual cortex (Fig. 1*A*). Because prolonged depolarization can affect inhibitory transmission (20), experiments were performed at −70 mV by using symmetric Cl^- solutions (16). First, we investigated the properties of single inhibitory synapses and measured miniature IPSCs (mIPSCs; Fig. 1*B*). mIPSCs occurred at similar frequencies, amplitudes, and kinetics in both genotypes (Fig. 1 *B* and *C*). Thus, unitary GABAergic transmission is not affected by the loss of Cx36. This notion is supported by quantitative PCR (qPCR) showing that GABA receptor subunit mRNA levels are similar in KOs and controls (Fig. S1).

We next evaluated the effects of Cx36KO on the inhibitory network. We blocked glutamatergic transmission, electrically stimulated L4, and measured evoked IPSCs in postsynaptic neurons. Stimulation activated multiple inhibitory neurons and evoked a compound IPSC (eIPSC) in the recorded cell (Fig. 1*D*). The eIPSC represents a summation of IPSCs from the activation of multiple interneurons and increased with increasing stimulation intensity before saturating (Fig. 1 *D* and *E*). The maximal eIPSCs, which is a measure of the total GABAergic inputs converging onto neurons, were similar between control and KO

Author contributions: F.P., C.-H.L., H.-K.L., and P.O.K. designed research; F.P., C.-H.L., C.D., M.K., H.-K.L., and P.O.K. performed research; D.P. and P.O.K. contributed new reagents/analytic tools; F.P., C.-H.L., H.-K.L., and P.O.K. analyzed data; and F.P., C.-H.L., H.-K.L., D.P., and P.O.K. wrote the paper.

The authors declare no conflict of interest.

*This Direct Submission article had a prearranged editor.

[1]F.P. and C.-H.L. contributed equally to this work.

[2]To whom correspondence should be addressed. E-mail: pkanold@umd.edu.

This article contains supporting information online at www.pnas.org/lookup/suppl/doi:10.1073/pnas.1100166108/-/DCSupplemental.

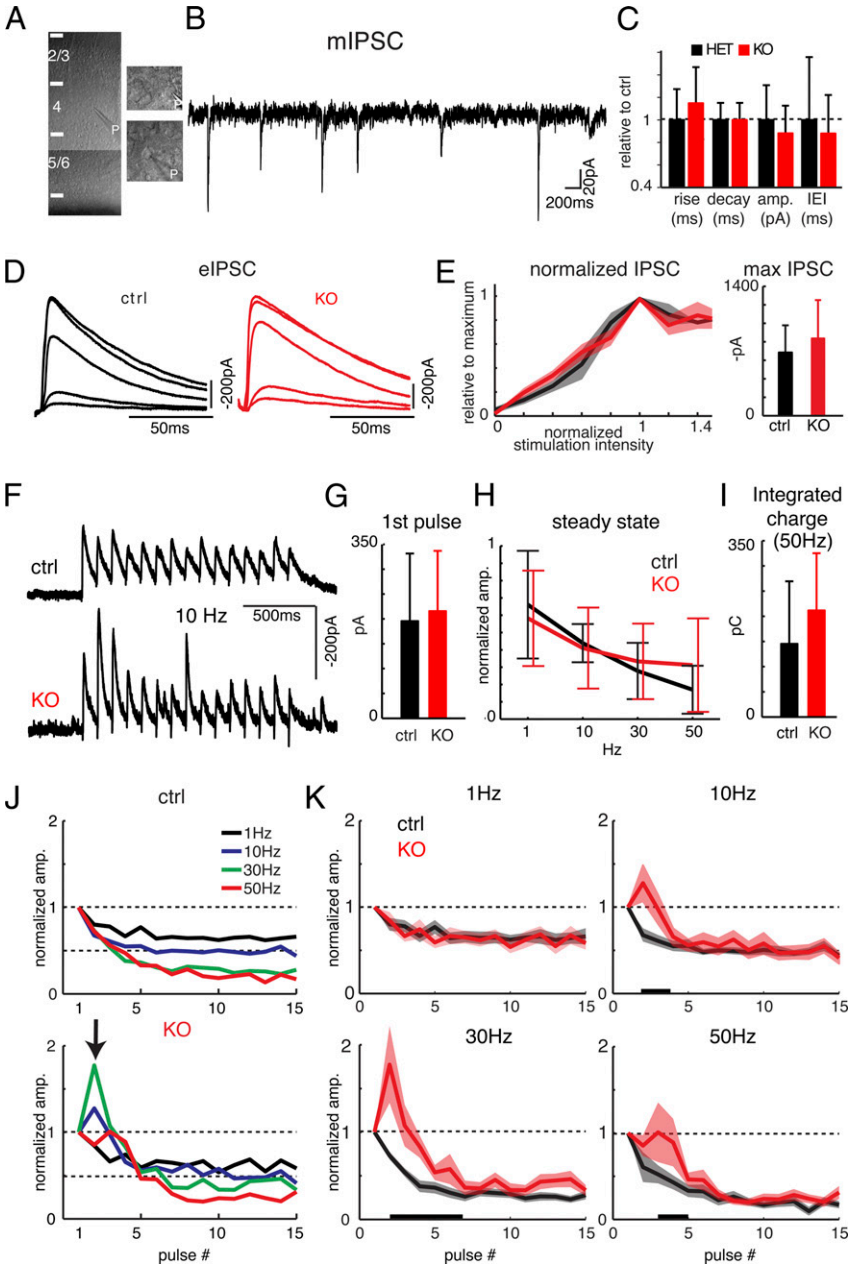

Fig. 1. Cx36-mediated synchronization alters evoked cortical IPSCs. (*A*) Low-magnification picture of recording location in L4 and high-magnification pictures of two recorded cells. P, patch pipette. (*B*) mIPSCs, recorded in the presence of TTX and glutamate blockers. (*C*) mISPCs were similar between control (n = 19) and KO (n = 18) (rise time: 4.2 ± 1.1 ms vs. 4.8 ± 1.3 ms; decay time: 21.4 ± 3.2 ms vs. 23.2 ± 4.3 ms; amplitude: 50.8 ± 15.7 pA vs. 44.8 ± 12.5 pA; interevent interval: 619 ± 345 ms vs. 544 ± 211 ms; all $P > 0.1$). Plotted are values normalized to mean control. (*D*) eIPSCs elicited by L4 stimulation at various stimulation intensities. (*E*) eIPSCs as function of stimulus level (normalized to maximum eIPSC in each cell). Plotted are mean ± SEM (thick line and shading) in bins of 0.2. Maximum eIPSC is similar in KO and control (661 ± 305 pA vs. 700 ± 432 pA; n = 8 and 13; $P > 0.1$). (*F*) eIPSCs in KO and control cells during 10-Hz trains. (*G*) eIPSC amplitude at first pulse is similar (195 ± 135 pA vs. 215 ± 121pA; n = 10 and 12; $P > 0.1$). (*H*) Steady-state eIPSC amplitudes for all stimulus frequencies (normalized to first pulse) are similar ($P > 0.1$). (*I*) Integrated charge over all stimulation pulses for 50-Hz stimulation is similar (145 ± 124 vs. 211 ± 113 pC; $P > 0.1$). (*J*) Mean eIPSC amplitudes at the first 15 pulses (normalized to eIPSC at first stimulus). In control eIPSCs depress. In KO the eIPSC facilitates at the second pulse for 10 and 30 Hz (arrow). (*K*) Mean eIPSCs for different stimulation frequencies. Shading indicates mean ± SEM. For 1 Hz, eIPSC amplitudes were similar in control and KO ($P > 0.05$; two-way ANOVA). For 10, 30, and 50 Hz, eIPSC amplitudes were different between control and KO ($P < 0.05$; two-way ANOVA; black bars).

cells (Fig. 1*E*). This result suggests that neurons in Cx36KO and control receive a comparable number of inhibitory inputs. The effects of gap junctional coupling on the network, however, might only be effective and revealed at submaximal stimulation intensities. To assess this possibility, we recorded IPSCs evoked with submaximal stimulation before and after application of the gap junction blocker carbenoxalone (CBX). CBX reduced eIPSC amplitudes in both genotypes but to a lesser degree in Cx36KO (Fig. S2). Although CBX has nonspecific effects (21) and potentially also blocks non-Cx36-containing gap junctions, the larger decrease in control suggests that a fraction (~25%) of the CBX-induced reduction in eIPSC amplitude is specific to gap junctions containing Cx36. Because coupling between inhibitory neurons enhances their synchrony (2–5), the eIPSC fraction mediated by Cx36 could be due to postsynaptic summation of synchronous IPSCs. This result is consistent with in vivo results showing that Cx36 removal reduces the amplitude of inhibition (8).

Because the removal of Cx36 also results in longer-lasting inhibition in vivo (8), and because Cx36 enhances the synchrony between inhibitory neurons (2–5), we next investigated the dynamic properties of inhibition. Inhibitory transmission is attenuated during repetitive activation, and this attenuation is thought to be due to vesicle depletion (16, 22, 23). Because Cx36 enables synchronous firing of inhibitory neurons, the lack of Cx36 in KOs might affect adaptation during repetitive stimulation. Therefore, we studied the inhibitory response of L4 cells to trains of stimulation pulses delivered at different frequencies (50, 30, 10, and 1 Hz; Fig. 1*F*). Stimulus intensities that produced similar eIPSC amplitudes during the first pulse between the two genotypes were chosen for the comparison (Fig. 1*G*). During the stimulus trains, eIPSC amplitude rapidly decreased until it reached a steady level, the amplitude of which was inversely related to the stimulation frequencies (Fig. 1 *E* and *G*). The amount of reduction at the steady state for all frequencies tested and the total charge transferred at 50 Hz were similar in both genotypes, suggesting that

loss of Cx36 does not cause major deficits in the synthesis of GABA and its source of readily releasable vesicles (Fig. 1 *G–I*). Although the steady-state levels were similar, we observed changes in the temporal properties of inhibitory transmission during stimulus trains. At a repetition rate of 1 Hz, amplitudes were similar between genotypes (Fig. 1*J*), but at higher stimulation frequencies, amplitudes were larger in Cx36KOs than controls for the first couple of stimulus pulses (Fig. 1*J*). In particular, in Cx36KO, eIPSCs at the second pulse of the 10- and 30-Hz pulse trains were larger than at the first pulse, thus displaying facilitation that was not observed in control (Fig. 1*J*). In addition, the normalized amplitudes at the subsequent 3–6 pulses for 10- to 50-Hz stimuli were larger in Cx36KO than in control (Fig. 1*K*). Thus, during high-frequency discharge, inhibition is more effective in Cx36KO within a time window of 30–100 ms (Fig. 1*K*). The facilitatory response observed in Cx36KO is reminiscent of reduced synaptic release, consistent with a Cx36-dependent component of the eIPSC (Fig. S2). Together, these in vitro results suggest that the removal of Cx36 results in initially weaker but longer-lasting inhibition, consistent with in vivo observations (8).

Cx36 Affects Synaptic Plasticity. Our in vitro results suggest that temporal dynamics of inhibition is altered in the Cx36KO. Altered inhibition can affect the function of the whole cortical network, and it has been shown to interfere with long-term synaptic plasticity (16). Thus, we investigated whether removal of Cx36 compromises LTD and LTP in layer 2/3 (L2/3; ref. 24). LTP was induced by TBS of L4, whereas LTD was induced by stimulating at a low frequency (1 Hz). We compared baseline amplitudes of local field potentials (LFPs) to postinduction (0–60 min) LFP amplitudes. After low-frequency stimulation, slices from all genotypes showed comparable reduction in LFP amplitudes (Fig. 2*A*). These results suggest that that Cx36 removal does not affect LTD.

TBS led to increased LFP amplitudes in WT slices (112.3 ± 8.3%; $P < 0.01$; $n = 8$ slices; $n = 3$ animals; Fig. 2*B*). In contrast, Cx36KO slices ($n = 10$ slices; $n = 6$ mice) did not show LFP amplitude increases ($P < 0.05$), but instead showed a trend to decrease (94.9 ± 8.5%; $P < 0.09$; Fig. 2*B*). The mean LFP amplitude after LTP in both WT and HET controls was significantly larger than in Cx36KO ($P < 0.0001$ and $P < 0.04$, respectively; Fig. 2*D*), but LFP increases in HETs showed more scatter and slightly lower mean increases than in WT (Fig. 2*B*). These data suggest that removal of Cx36 prevents synaptic strengthening with high-frequency stimuli. In contrast, the ability of synapses to undergo synaptic weakening with low-frequency stimuli does not depend on Cx36.

The deficits in TBS-LTP could be due to intrinsic deficits in synaptic plasticity. We thus investigated whether pairing LTP was present in Cx36KOs. L2/3 neurons were recorded via whole-cell patch clamp, and pairing LTP was induced by pairing 0 mV depolarization with low-frequency stimulations (1 Hz, 200 pulses). Both WT and Cx36KOs exhibited comparable pairing LTP ($P = 0.635$; Fig. 2*C*). Thus, together our results suggest that, although excitatory synapses retain the capability of expressing LTP, the induction of LTP with high-frequency stimuli is selectively impaired.

The deficits in TBS-LTP could potentially be due to altered glutamatergic signaling. To explore this possibility, we obtained recordings from L2/3 neurons under conditions that evoke isolated AMPA or NMDA currents (Fig. 3*A*). Neither the ratio of AMPA-to-NMDA currents (Fig. 3*A*) nor NMDA current decay times, which depend on the proportion of NR2A and NR2B subunits (25, 26), showed any significant difference between genotypes (Fig. 3*B*). Consistent with these observations, we found similar levels of NR2A and NR2B mRNAs in Cx36KOs and controls (Fig. 3*C*). Therefore, the absence of Cx36 in neuronal networks does not grossly influence excitatory transmission or intrinsic plasticity mechanisms. However, we found that the responses during the TBS suppressed more in the KOs compared with HETs and WTs, which was quantified by comparing the

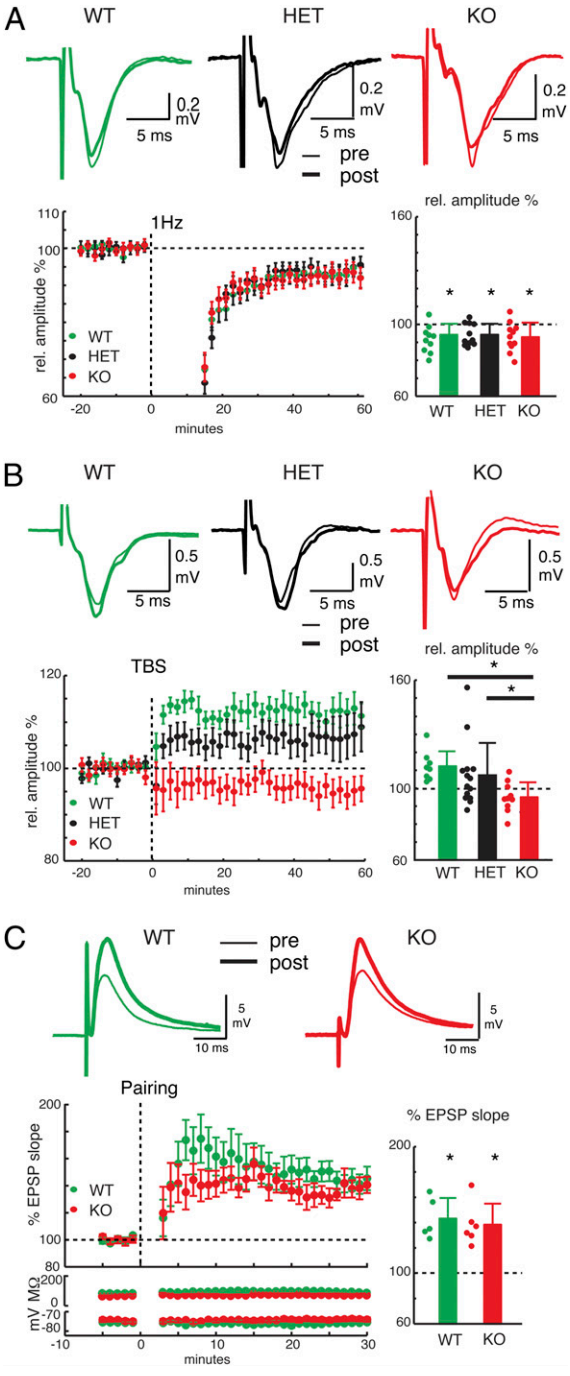

Fig. 2. TBS LTP, but not LTD, is impaired in Cx36KO. (*A Upper*) Plotted are field potential (LFP) amplitudes before and after application of 1-Hz stimulus. (*Lower*) Time course of LTD and relative LFP amplitudes after 60 min. Filled circles indicate individual slices. The reduction in LFP amplitudes was similar (KO: 94.3 ± 6.1%, 11 slices, 6 animals; HET: 92.2 ± 8.0%, 11 slices, 6 animals; WT: 92.9 ± 7.8 12 slices, 2 animals; all $P < 0.05$,'*'). (*B Upper*) Plotted are LFP amplitudes before and after application of TBS stimulus. (*Lower*) Time course of LTP and relative LFP amplitudes (rel. to baseline) after 60 min. *$P < 0.05$. (*C*) Paring LTP. Traces show whole cell EPSPs in L2/3 neurons before and after pairing stimulation. (*Lower*) Time course of LTP. Plotted is % EPSP slope before and after pairing in WT and KO. Lower graphs show input resistance and membrane potential. Bar graph shows %EPSP slope after 30 min in WT (143 ± 7.2%; 5 cells, 4 animals; $P < 0.004$) and KOs (138 ± 6.8%; 6 cells, 5 animals; $P < 0.003$). Filled circles indicate individual cells.

normalized LFP area during the TBS (Fig. 3*D*). This result is consistent with an interpretation that there is enhanced inhibition during TBS in the KOs, because the degree of frequency depression in L2/3 of visual cortex depends on the strength of inhibition (27). This result is also consistent with the frequency facilitation of eIPSCs seen in Cx36KO (Fig. 1 *J* and *K*).

Cx36 Regulates OD Plasticity. Our in vitro results reveal specific deficits in temporal profile of inhibitory efficacy and synaptic plasticity in Cx36KO. Both inhibitory efficacy and synaptic plasticity are important for normal developmental refinement and plasticity of cortical organization (1, 17). Thus, we investigated whether OD plasticity of visual cortex requires the presence of Cx36 (Fig. 4*A*). We chronically recorded visually evoked potentials (VEPs) in the binocular zone (BZ) of the primary visual cortex to measure the input strength of both ipsilateral and contralateral eyes before and after 5–6 d of MD. After 2 d of habituation, baseline VEPs were obtained in response to stimulation of each eye (Fig. 4*B*). To circumvent the effects of Cx36KO on rod photoreceptor signaling (19), we recorded VEPs under photopic illumination, which activates cone photoreceptors (>50 cd/m^2). Baseline VEP waveforms (Fig. 4*B*) and amplitudes (Fig. 4*C*, pre) at P25 were similar in Cx36KOs and controls. Thus, the initial development of OD does not require Cx36.

Next, we induced OD shifts by monocularly depriving animals for 5–6 d through the contralateral eyes starting at ~P25 (Fig. 4*D*, post). OD plasticity varies between mouse strains (28). Because Cx36KOs are kept on a mixed background (*Methods*), we used both WT and HET littermates as controls. In control mice, we observed the expected reduction in VEP amplitude to DE stimulation and increase of VEP amplitude to NDE stimulation (Fig. 4 *D* and *E*). We evaluated the OD shift by calculating the difference in the DE/NDE VEP ratios (Fig. 4*F*). A reduction of the ratio after MD indicated a shift in OD toward the NDE. In control animals, we observed a reduction in the ratio, indicating the expected OD shift toward the NDE (13). In contrast, Cx36KOs displayed reduced VEP amplitudes after stimulation of either NDE or DE (Fig. 4 *D* and *E*), which manifested as no change in OD ratio after MD (Fig. 4*F*). The abnormal NDE weakening (Fig. 4*E*) therefore undermined OD plasticity in Cx36KOs (Fig. 4*F*).

Although VEP recordings detect physiological changes in the relative strength of both eyes caused by MD, they do not reveal changes in the spatial extent of the functional representation of both eyes that typically accompany OD plasticity, i.e., the expansion of regions responding to the NDE or contraction of regions responding to the DE. To explore this issue, we measured the expression of *Arc*, an immediate early gene that is rapidly expressed in visual cortical neurons after brief visual stimulation (11, 29–31) with in situ hybridization. The visually induced expression pattern of *Arc* is a sensitive indicator of OD plasticity in both mice and cats (11, 29–31). As expected, after monocular enucleation (ME) in control, the functional representation of the NDE increased in control (Fig. S3). In contrast, no discernible expansion in the functional NDE representation after ME was detected in Cx36KO, and the reduced *Arc* expression intensity suggests a weakening of the NDE-driven activity (Fig. S3). Together with the VEP data, these results show that Cx36 is required for normal OD plasticity.

The abnormal OD plasticity in Cx36KO might be due to the enhanced frequency facilitation of IPSCs, which is a consequence of a reduction in release. Hence, enhancing GABA release might rescue OD plasticity. CB1 endocannabinoid receptors (CB1Rs) are expressed in electrically coupled interneurons (32) and regulate IPSC amplitudes by affecting GABA release. CB1 activation decreases IPSC amplitudes by lowering GABA release, whereas blocking CB1 has the opposite effect (33–35). Moreover, increasing GABA release by blocking CB1 decreases frequency facilitation (36). Thus, we blocked CB1R with the selective antagonist AM251 and reassessed OD plasticity. First, we investigated whether AM251 injection by itself had any effect. Injections of AM251 in unmanipulated animals did not alter VEP amplitudes in either genotype (Fig. S4). Furthermore, MD in control animals concurrent with AM251 injections produced normal OD shifts (Fig. 4 *E* and *F* and Fig. S4), consistent with previous results (37). In contrast, AM251 treatment on Cx36KOs recovered normal OD shifts after MD (Fig. 4 *E* and *F* and Fig. S4). The restoration of OD plasticity in Cx36KOs by AM251 was due to a rescue of NDE strengthening, as evidenced by increased NDE VEP amplitudes after MD (Fig. 4 *E* and *F*). Together, these data support the idea that the altered OD plasticity in Cx36KOs is the result of abnormal inhibition.

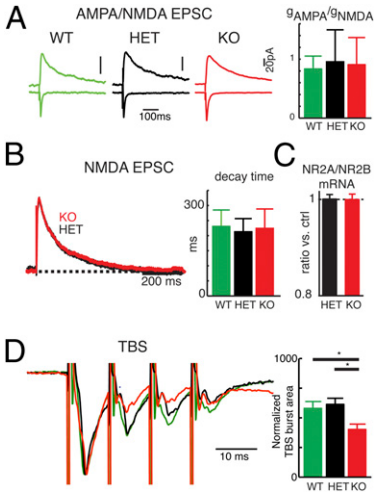

Fig. 3. Normal AMPA and NMDA function in Cx36KO. (*A*) Evoked AMPA and NMDA EPSCs in L2/3 neurons measured by holding cell by -70 and +40 mV, respectively. AMPA/NMDA conductance ratios were similar between genotypes (0.83 ± 0.22, 0.95 ± 0.55, 0.91 ± 0.46; n = 6, 10, and 16, respectively; $P > 0.1$; ANOVA). (*B*) Representative traces of evoked NMDA currents scaled to peak amplitude. Average NMDA EPSC decay-times were similar between genotypes (231 ± 54 ms, 213 ± 44 ms, 224 ± 64 ms; $P > 0.1$; ANOVA). (*C*) RNA levels of NMDA receptor subunits NR2A and NR2B obtained with qRT-PCR. Normalized mRNA ratios were similar between genotypes (1.0 ± 0.01 vs. 0.99 ± 0.016; n = 9, control, and n = 5, KO; $P > 0.1$; t test). (*D*) Responses during TBS in the different genotypes. The normalized LFP area during the TBS was more suppressed in the KOs compared with HET and WT [WT = 580 ± 57.5, n = 8; HET = 614 ± 51.3, n = 14; KO = 402 ± 44.6, n = 10; ANOVA: $F(2, 29) = 5.511$; $P < 0.01$].

Discussion

Our studies show that Cx36 signaling in inhibitory neurons is required for normal LTP and OD plasticity. A major difference between control and Cx36KO on a synaptic level is that high-frequency stimuli, such as TBS, that normally evoke LTP fail to do so in Cx36KO. The synaptic effect of Cx36KO is reflected in vivo by a change in response to MD. After MD, NDE inputs to the visual cortex weaken rather than strengthen as they do in control. The physiological data are consistent with the *Arc* induction results. *Arc* induction showed that the NDE increase is almost absent in Cx36KO and that *Arc* intensity of the remaining region driven by the NDE is reduced. This result suggests a net decrease of NDE-driven activity in Cx36KOs. Thus, in Cx36KO, MD leads to a weakening of both eyes and therefore does not lead to a net shift of OD toward the NDE.

Our results suggest that the effects of Cx36 deletion on LTP and OD plasticity are not due to gross deficiencies in glutamatergic transmission or mechanisms of synaptic plasticity. However, we found a specific impairment of inhibition in the absence of Cx36. Our data show facilitatory responses to high-frequency stimulation. Thus, inhibition is longer lasting in the absence of Cx36. Because our stimulation protocol was adjusted to normalize the IPSC amplitude of the first pulse of a stimulus

NEUROSCIENCE

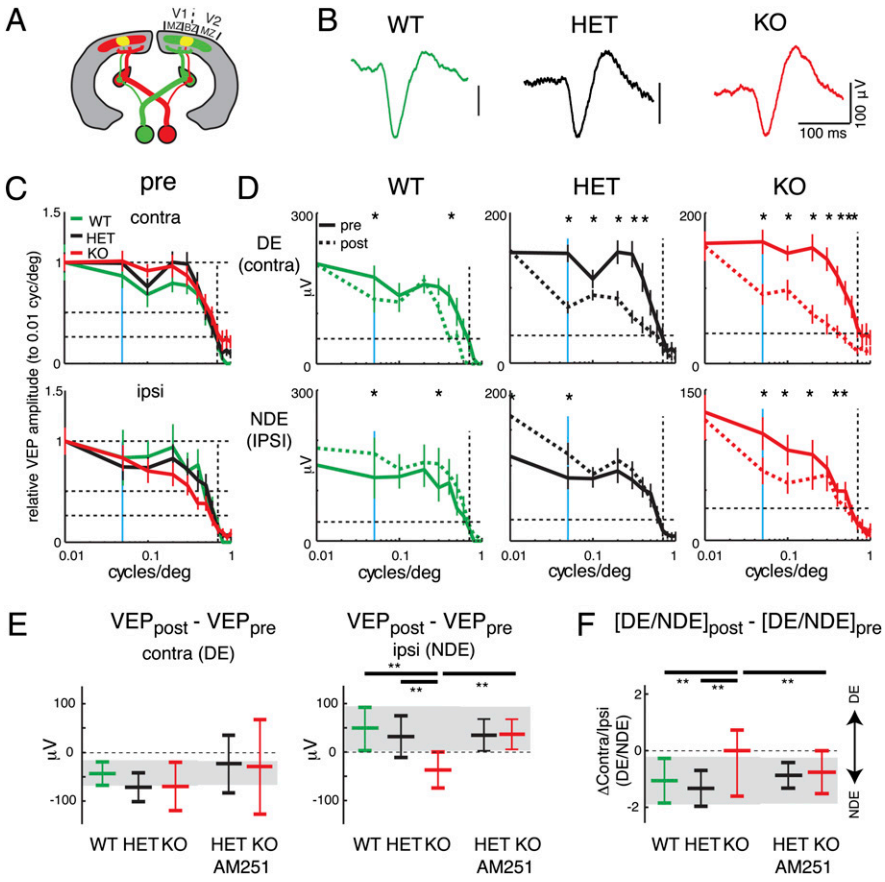

Fig. 4. Impaired OD plasticity in Cx36KO mice. (*A*) Mouse visual cortex consists of a large monocular zone (MZ), where neurons are visually responsive exclusively to stimulation of the contra eye, and a smaller binocular zone (BZ), in which inputs from both eyes converge. (*B*) Waveforms of VEPs display no obvious difference between genotypes. VEP amplitude is the difference between peaks. (*C*) VEP amplitudes to stimulation of ipsi and contra eye at different spatial frequencies relative to 0.01 cycles per degree. Plotted are means ± SD. Horizontal lines indicate 100%, 50%, and 25% and vertical lines indicate spatial frequencies of 0.05 (blue) and 0.5 (dashed) cycles per degree. VEP amplitudes before (pre) MD did not differ significantly ($P > 0.1$; one-way ANOVA) in WT ($n = 6$), HET ($n = 11$), and KO ($n = 10$) for stimulus of either eye. (*D*) Effect of contra eye MD. Plotted are mean VEP amplitudes before (pre, solid lines) and after (post, dashed lines) MD. In WT and HET, DE responses are reduced (*$P < 0.05$; paired *t* test), whereas NDE inputs strengthen (*$P < 0.05$; paired *t* test). Both DE and NDE inputs weaken in KO (*$P < 0.05$; paired *t* test). (*E*) Change in VEP amplitudes pre- and post-MD at 0.05 cycles per degree. Horizontal bars indicate means and SD. Gray box, mean ± 1 SD of WT. The change in DE and NDE VEP amplitudes was similar in all genotypes ($P > 0.05$; ANOVA). The change in NDE amplitude in KO was different from both WT and HET (**$P < 0.005$; ANOVA). There were slight differences in the amount of DE weakening between WT and HET, which might reflect strain background or gene dosage effects. Similar to our observations on LTP, these differences were not significant. Chronic application of AM251 did not alter the change in the DE for both genotypes and the NDE for HET. However, AM251 application rescued NDE strengthening in KO ($P < 0.05$). (*F*) Plotted is the difference in contra/ipsi (DE/NDE) VEP amplitude ratio (post-MD– pre-MD) at 0.05 cycles per degree. A negative shift indicates shift toward the NDE. Control animals shift toward the NDE ($P < 0.05$). In contrast to both WT and HET animals (**$P < 0.005$; ANOVA), the OD ratio in KO did not shift ($P > 0.05$). Application of AM251 did not affect OD shifts in HET, but rescued the OD shift in KO ($P < 0.05$).

train, we did not observe large differences in IPSC amplitude between cells. However, our pharmacological manipulations showed that a fraction (~25%) of the eIPSC is due to coupling via Cx36, given the lower efficacy of CBX in the Cx36KO. This result is consistent with in vivo results, which showed that removal of Cx36 leads to reduced inhibitory amplitudes and prolonged duration of inhibition (8). At a single synapse, the postsynaptic amplitude depends on the probability of synaptic release (p_s), the evoked amplitude of the transmitter contained in a synaptic vesicle (a_s), and the number of vesicles released (n): $A_s = p_s{}^*n{}^*a_s$. In a network with independently acting neurons, the compound amplitude (A_n) depends on the single neuron firing probability (p_n), the evoked amplitude A_s, and the number of neurons (m): $A_n = p_n{}^*A_s{}^*m = p_n{}^*m{}^*p_s{}^*n{}^*a_s$. Thus, the release probability of the network (p_{rn}) depends on both p_n and p_s, as: $p_{rn} = p_n{}^*p_s$. Our data are consistent with decreased p_{rn}. Desynchronization reduces p_n and thereby p_{rn}. Thus, a facilitating network response in Cx36KO is consistent with reduced activation of the inhibitory network for low-frequency inputs and an increased facilitation for a brief time window (~30–100 ms) during high-frequency stimulation. AM251 increases synaptic release probability (p_s), which can then increase p_{rn}. Consistent with this scenario, our results show that AM251 injections rescue OD plasticity in Cx36KO.

How, then, do these deficits in inhibition in Cx36KO relate to the observed changes in LTP and OD plasticity? Altered temporal profile of inhibitory efficacy can alter timing relationships between thalamic and cortical activity consistent with reduced gamma activity in Cx36KO (8, 38, 39). Such altered timing relationships can alter synaptic plasticity. For example, in studies where thalamic inputs to visual cortex were experimentally decorrelated from cortical neurons by cortical silencing, NDE weakening was also observed (40–42). Altered inhibitory efficacy can produce LTP deficits through multiple mechanisms. Most likely, enhanced inhibition during high-frequency stimulation may attenuate NMDA receptor activation and, consequently, LTP (27). Consistent with this scenario, we showed that Cx36KOs display increased inhibition (within a window of 30–100 ms) and stronger suppression of excitatory responses during repetitive high-frequency stimulation.

In Cx36KO, the coding region for Cx36 was replaced with β-gal and alkaline phosphatase. Thus, as a sensitive control for possible effects of reporter gene expression, we compared KO cells to their HET counterparts (18, 19). Electrical coupling in thalamic reticular nucleus neurons from Cx36 HET is qualitatively similar to WT (18), but effects of gene dosage on connexin levels have been reported for other connexins (43). Although effects of MD on OD plasticity were largely similar in WT and HET, we observed slight differences in LTP between both groups. Thus, the differences in LTP we observed in HET could be related to gene dosage effects and a higher sensitivity of LTP to slight perturbations in coupling. Regardless, the difference between WT and HET responses after LTP did not reach statistical significance, whereas the difference between control and Cx36KO did.

The notion that an alteration in the overall levels of inhibition accounts for the impaired OD plasticity in the Cx36KO is well supported. Our results are consistent with the view that a certain level of inhibition is required for OD plasticity to occur (1). For example, knockout of the 65-kD isoform of the GABA synthetic enzyme glutamic acid decarboxylase (GAD65) impairs OD plas-

ticity and LTD and causes deregulation of NMDA receptor levels (16, 31, 44). We show that removal of Cx36 impairs OD plasticity and LTP. Thus, our results extend the previous model by showing that inhibition can affect either LTP or LTD and that in both cases OD plasticity is impaired. Our results also show that the strength and dynamic properties of inhibition can be regulated by at least two complementary pathways: synchrony of inhibitory neurons via Cx36 and GABA production/release via GAD65.

Modulation of the strength and dynamic properties of inhibition by synchronizing the output of coupled neurons has distinct advantages over other known mechanisms for regulation of synaptic strength. Several neurons synchronizing their output on a single target neuron constitutes a form of gain control, which can be dynamically modulated in vivo by activity-dependent mechanisms on a second-to-minute time scale (45). This finding complements other mechanisms, such as altered levels of receptor expression, that operate on timescales of minutes to days. Regardless of whether or not such temporal factors play a role in inhibition, our results demonstrate that electrical coupling between inhibitory interneurons has profound effects on the temporal dynamics of inhibition and is critical for normal OD plasticity.

Methods

See *SI Methods* for detailed methods. Experiments were conducted in accordance with the Animal Care and Use Committees of the University of Maryland and Harvard Medical School. Cx36KO mice were generated as described (6). Slice electrophysiology was performed as described (24, 31). To record EPSCs, pipettes were filled with a cesium-based solution. AMPA and NMDA EPSCs were isolated by holding neurons at −70 and +40 mV, respectively, and blocking GABAergic transmission. IPSCs were isolated by blocking glutamate receptors. To measure IPSCs at −70mV, the reversal potential of Cl^- was shifted to 0 mV (16). Field potentials were recorded as described (46, 47). For pairing LTP, neurons were recorded in current clamp, and evoked eEPSPs were monitored by stimulation of L4. Pairing LTP was induced by switching to voltage clamp, holding the neurons to 0 mV, and stimulating at 1 Hz (200 pulses). VEP recordings were performed in awake, head-restrained mice by using chronically implanted microelectrodes (37). Electrodes were implanted into L4 of the right hemisphere between P22 and P25. VEPs were elicited by using full-field sine-wave gratings. For MD experiments, eyes were reopened and tested by using stimuli oriented perpendicular to the baseline stimuli. OD ratio was computed as contra/ipsi VEP amplitude ratio. OD plasticity experiments using *Arc* and qRT-PCR were carried out as described (11, 29–31, 48). ANOVA, *t* test, or Wilcoxon was used for statistical comparisons, and $P < 0.05$ was considered significant.

ACKNOWLEDGMENTS. We thank the laboratory of Dr. Carla Shatz for technical support with the *Arc* in situ hybridizations. P.O.K. is supported by a Ralph E. Powe Award and National Institutes of Health (NIH) Grants R21DC009454 and R01DC009607. D.P. is supported by NIH Grants R01EY014127 and R01GM37751. H.-K.L. is supported by NIH Grant R01EY014882.

1. Hensch TK (2004) Critical period regulation. *Annu Rev Neurosci* 27:549–579.
2. Buzsáki G (2001) Electrical wiring of the oscillating brain. *Neuron* 31:342–344.
3. Beierlein M, Gibson JR, Connors BW (2000) A network of electrically coupled interneurons drives synchronized inhibition in neocortex. *Nat Neurosci* 3:904–910.
4. Gibson JR, Beierlein M, Connors BW (1999) Two networks of electrically coupled inhibitory neurons in neocortex. *Nature* 402:75–79.
5. Liu XB, Jones EG (2003) Fine structural localization of connexin-36 immunoreactivity in mouse cerebral cortex and thalamus. *J Comp Neurol* 466:457–467.
6. Deans MR, Gibson JR, Sellitto C, Connors BW, Paul DL (2001) Synchronous activity of inhibitory networks in neocortex requires electrical synapses containing connexin36. *Neuron* 31:477–485.
7. Van Der Giessen RS, et al. (2008) Role of olivary electrical coupling in cerebellar motor learning. *Neuron* 58:599–612.
8. Butovas S, Hormuzdi SG, Monyer H, Schwarz C (2006) Effects of electrically coupled inhibitory networks on local neuronal responses to intracortical microstimulation. *J Neurophysiol* 96:1227–1236.
9. Wiesel TN, Hubel DH (1963) Single-cell responses in striate cortex of kittens deprived of vision in one eye. *J Neurophysiol* 26:1003–1017.
10. Hubel DH, Wiesel TN, LeVay S (1977) Plasticity of ocular dominance columns in monkey striate cortex. *Philos Trans R Soc Lond B Biol Sci* 278:377–409.
11. Tagawa Y, Kanold PO, Majdan M, Shatz CJ (2005) Multiple periods of functional ocular dominance plasticity in mouse visual cortex. *Nat Neurosci* 8:380–388.
12. Sawtell NB, et al. (2003) NMDA receptor-dependent ocular dominance plasticity in adult visual cortex. *Neuron* 38:977–985.
13. Frenkel MY, Bear MF (2004) How monocular deprivation shifts ocular dominance in visual cortex of young mice. *Neuron* 44:917–923.
14. Gordon JA, Stryker MP (1996) Experience-dependent plasticity of binocular responses in the primary visual cortex of the mouse. *J Neurosci* 16:3274–3286.
15. Hensch TK, Stryker MP (1996) Ocular dominance plasticity under metabotropic glutamate receptor blockade. *Science* 272:554–557.
16. Choi SY, Morales B, Lee HK, Kirkwood A (2002) Absence of long-term depression in the visual cortex of glutamic acid decarboxylase-65 knock-out mice. *J Neurosci* 22:5271–5276.
17. Smith GB, Heynen AJ, Bear MF (2009) Bidirectional synaptic mechanisms of ocular dominance plasticity in visual cortex. *Philos Trans R Soc Lond B Biol Sci* 364:357–367.
18. Landisman CE, et al. (2002) Electrical synapses in the thalamic reticular nucleus. *J Neurosci* 22:1002–1009.
19. Deans MR, Volgyi B, Goodenough DA, Bloomfield SA, Paul DL (2002) Connexin36 is essential for transmission of rod-mediated visual signals in the mammalian retina. *Neuron* 36:703–712.
20. Alger BE, Pitler TA (1995) Retrograde signaling at GABAA-receptor synapses in the mammalian CNS. *Trends Neurosci* 18:333–340.
21. Tovar KR, Maher BJ, Westbrook GL (2009) Direct actions of carbenoxolone on synaptic transmission and neuronal membrane properties. *J Neurophysiol* 102:974–978.
22. Varela JA, Song S, Turrigiano GG, Nelson SB (1999) Differential depression at excitatory and inhibitory synapses in visual cortex. *J Neurosci* 19:4293–4304.
23. Galarreta M, Hestrin S (1998) Frequency-dependent synaptic depression and the balance of excitation and inhibition in the neocortex. *Nat Neurosci* 1:587–594.
24. Goel A, et al. (2006) Cross-modal regulation of synaptic AMPA receptors in primary sensory cortices by visual experience. *Nat Neurosci* 9:1001–1003.
25. Philpot BD, Sekhar AK, Shouval HZ, Bear MF (2001) Visual experience and deprivation bidirectionally modify the composition and function of NMDA receptors in visual cortex. *Neuron* 29:157–169.
26. Quinlan EM, Philpot BD, Huganir RL, Bear MF (1999) Rapid, experience-dependent expression of synaptic NMDA receptors in visual cortex in vivo. *Nat Neurosci* 2:352–357.
27. Rozas C, et al. (2001) Developmental inhibitory gate controls the relay of activity to the superficial layers of the visual cortex. *J Neurosci* 21:6791–6801.
28. Heimel JA, Hermans JM, Sommeijer JP, Levelt CN; Neuro-Bsik Mouse Phenomics consortium (2008) Genetic control of experience-dependent plasticity in the visual cortex. *Genes Brain Behav* 7:915–923.
29. Syken J, Grandpre T, Kanold PO, Shatz CJ (2006) PirB restricts ocular-dominance plasticity in visual cortex. *Science* 313:1795–1800.
30. Datwani A, et al. (2009) Classical MHCI molecules regulate retinogeniculate refinement and limit ocular dominance plasticity. *Neuron* 64:463–470.
31. Kanold PO, Kim YA, GrandPre T, Shatz CJ (2009) Co-regulation of ocular dominance plasticity and NMDA receptor subunit expression in glutamic acid decarboxylase-65 knock-out mice. *J Physiol* 587:2857–2867.
32. Galarreta M, Erdélyi F, Szabó G, Hestrin S (2004) Electrical coupling among irregular-spiking GABAergic interneurons expressing cannabinoid receptors. *J Neurosci* 24:9770–9778.
33. Földy C, Neu A, Jones MV, Soltesz I (2006) Presynaptic, activity-dependent modulation of cannabinoid type 1 receptor-mediated inhibition of GABA release. *J Neurosci* 26:1465–1469.
34. Katona I, et al. (1999) Presynaptically located CB1 cannabinoid receptors regulate GABA release from axon terminals of specific hippocampal interneurons. *J Neurosci* 19:4544–4558.
35. Kang-Park MH, Wilson WA, Kuhn CM, Moore SD, Swartzwelder HS (2007) Differential sensitivity of GABA A receptor-mediated IPSCs to cannabinoids in hippocampal slices from adolescent and adult rats. *J Neurophysiol* 98:1223–1230.
36. Jiang B, et al. (2010) The maturation of GABAergic transmission in visual cortex requires endocannabinoid-mediated LTD of inhibitory inputs during a critical period. *Neuron* 66:248–259.
37. Liu CH, Heynen AJ, Shuler MG, Bear MF (2008) Cannabinoid receptor blockade reveals parallel plasticity mechanisms in different layers of mouse visual cortex. *Neuron* 58:340–345.
38. Hormuzdi SG, et al. (2001) Impaired electrical signaling disrupts gamma frequency oscillations in connexin 36-deficient mice. *Neuron* 31:487–495.
39. Buhl DL, Harris KD, Hormuzdi SG, Monyer H, Buzsáki G (2003) Selective impairment of hippocampal gamma oscillations in connexin-36 knock-out mouse in vivo. *J Neurosci* 23:1013–1018.
40. Hata Y, Stryker MP (1994) Control of thalamocortical afferent rearrangement by postsynaptic activity in developing visual cortex. *Science* 265:1732–1735.
41. Hata Y, Tsumoto T, Stryker MP (1999) Selective pruning of more active afferents when cat visual cortex is pharmacologically inhibited. *Neuron* 22:375–381.
42. Rittenhouse CD, Shouval HZ, Paradiso MA, Bear MF (1999) Monocular deprivation induces homosynaptic long-term depression in visual cortex. *Nature* 397:347–350.
43. Huang GY, et al. (1998) Alteration in connexin 43 gap junction gene dosage impairs conotruncal heart development. *Dev Biol* 198:32–44.
44. Hensch TK, et al. (1998) Local GABA circuit control of experience-dependent plasticity in developing visual cortex. *Science* 282:1504–1508.
45. Landisman CE, Connors BW (2005) Long-term modulation of electrical synapses in the mammalian thalamus. *Science* 310:1809–1813.
46. Kirkwood A, Lee HK, Bear MF (1995) Co-regulation of long-term potentiation and experience-dependent synaptic plasticity in visual cortex by age and experience. *Nature* 375:328–331.
47. Kirkwood A, Rioult MC, Bear MF (1996) Experience-dependent modification of synaptic plasticity in visual cortex. *Nature* 381:526–528.
48. Kanold PO, Shatz CJ (2006) Subplate neurons regulate maturation of cortical inhibition and outcome of ocular dominance plasticity. *Neuron* 51:627–638.